

# MODELING OF TRIODE SOURCE OF INTENSE RADIAL CONVERGING ELECTRON BEAM

V. Altsybeyev \*, V. Engelko, A. Ovsyannikov, D. Ovsyannikov, V. Ponomarev  
 Saint-Petersburg State University, 7/9 Universitetskaya nab., St. Petersburg, 199034 Russia  
 R. Fetzer, G. Mueller  
 Karlsruhe Institute of Technology, Institute for Pulsed Power and Microwave Technology,  
 PO Box 3640, 76021 Karlsruhe, Germany

## Abstract

The considered source of triode type produces intense radial converging electron beam for irradiation of cylindrical targets. As an electron emitter an explosive plasma cathode is used. The role of initial transverse velocities of electrons, defocusing effect of the controlling grid, the beam self-magnetic field, electron and ion emission from the controlling grid, backscattering of electrons and ion flow from the target is analyzed. Conditions for achieving required electron beam parameters (the electron kinetic energy - 120 keV, the beam energy density on the target  $40 \text{ J/cm}^2$  on a maximum possible length of the target surface) were determined.

## INTRODUCTION

In ref.[1] the design of the electron source of triode type producing an intense radial converging electron beam employed for modification of the outer surface of cylindrical targets (such, for example, as fuel element claddings) is described. In this paper we performed the set of numerical simulations and try to analyze the following physical effects arising in the considered source: the role of the initial transverse velocity of electrons, defocusing effect of the controlling grid, the beam self-magnetic field, backscatter of electrons, ion flow from the target. Using obtained results one can determine the source parameters that ensures stable operation mode and conditions for achieving the required beam energy density on the target  $\sim 40 \text{ J/cm}^2$  per 40-60  $\mu\text{s}$  impulse. For numerical particle-in-cell simulations [2] the DAISI code will use [3-8].

## SCHEME OF THE SOURCE

The electron source consists of the outer cylindrical cathode, anode and controlling grid [1]. The values of the main parameters are presented in Table 1.

Table 1: Parameters of the Source

Cathode length, m	$L = 0.98 \text{ m}$
Cathode radius, m	$r_c = 0.15 \text{ m}$
Grid radius, m	$r_g = 0.1 \text{ m}$
Anode/Target radius, m	$r_a = 0.005 \text{ m}$
Cathode-grid voltage, V	$U_{cg} = 20 - 40 \text{ kV}$
Cathode-anode voltage, V	$U_{ca} = 80 - 140 \text{ kV}$

\* v.altsybeev@spsu.ru

In the new source design a multi-arc plasma cathode is applied. At such a cathode plasma is produced by a vacuum arc discharge provided by a large number of discharge gaps equally spaced on the cathode area. The space occupied by the plasma is separated from an external electric field by a separating grid. Such cathode design allows to control the value of the emission current density and to reduce the initial angular spread of electrons.

## STABLE AND UNSTABLE OPERATION MODES

We performed a set of simulations for different cathode-grid and cathode-anode voltages, for monopolar electron flow and bipolar electron and ion flows, for different grid electrode radius. Main results are the following. For each grid radius and cathode-anode voltage there is a critical value of the cathode-grid voltage  $U_{cr}$  dividing the mode of the source operation for stable and unstable regime (Fig. 1. As an example,  $U_{cr} = 25 \text{ kV}$  for the grid radius  $r_g = 0.1 \text{ m}$  and  $U_{ca} = 120 \text{ kV}$ . If  $U_{cg}$  is less than or equal to the critical value the source operates stably, electron and ion trajectories are laminar, currents reach their stable magnitudes within several tens of nanoseconds, and the distribution of the power density on the target length 0.75 m is sufficiently homogeneous, as it is seen from.

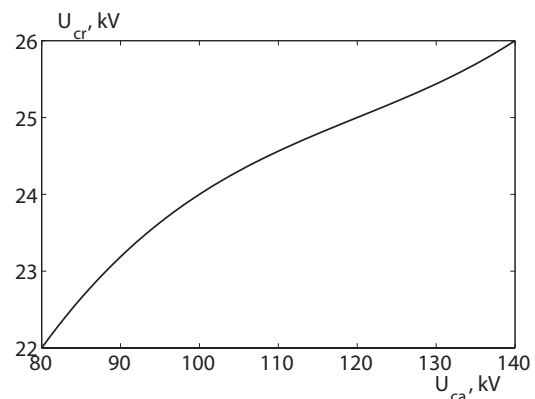


Figure 1: Dependence of  $U_{cr}$  on  $U_{ca}$  for  $r_g = 0.1 \text{ m}$ .

When the cathode-grid voltage exceeds the critical value the source operation is unstable, electron and ion currents do not reach stable magnitudes, particle flows are not laminar. Under the influence of the beam self magnetic field electrons move from the edges of the source to its central part, which leads to inhomogeneity of the power density

distribution on the target (Fig. 2). In addition, the structure of the power density distribution is different in different moments of time, which is the consequence of unstable source operation.

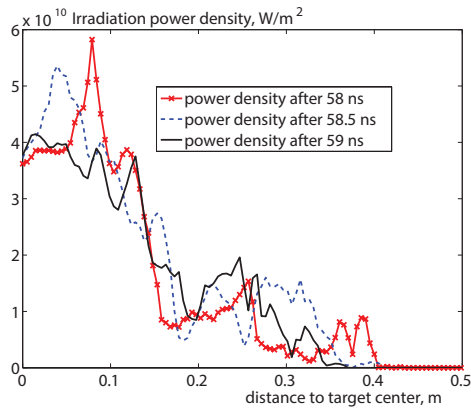


Figure 2: Power density on half of the target for different moments of time.  $U_{cg} = 40$  kV,  $U_{ca} = 120$  kV,  $r_g = 0.1$  m.

### THE ROLE OF THE TRANSVERSE VELOCITY OF ELECTRONS

Transverse velocity of electrons may be caused by the temperature of the cathode plasma or by the transverse electric field existing in the controlling grid region (108 wires with 0.2 mm in diameter). Let us consider first the grid effect. We performed simulations of electron beam dynamics in the source cross-section plane with taking into account real field distribution in the area of the controlling grid. In Fig. 3 an example of the potential distribution between wires is shown. One can see that the potential drop is rather small. Note, that the space charge of electrons slightly increases the potential drop while the space charge of ions decreases it. Fig. 4 illustrates the combined influence of the cathode plasma temperature and azimuthal electric field in the controlling grid region on the efficiency of the electron beam focusing to the target ( $I_e$  and  $I_t$  are electron emission current and current to the target correspondingly). Finally, calculations showed that the influence of the grid on the electron beam focusing can be neglected.

Calculations showed that the cathode plasma temperature significantly affects the source operation if  $T$  exceeds 30 eV. In particular, a part of electrons passes by the target and oscillates in the source volume (Fig. 5).

### CONDITIONS FOR ACHIEVING THE REQUIRED BEAM ENERGY DENSITY

We performed a set of simulations for different cathode plasma temperatures, with taking into account electron backscatter from stainless steel target [9, 10], ion flow from target and beam self-magnetic field.

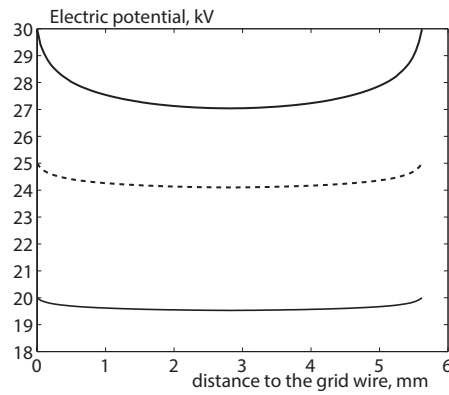


Figure 3: Distribution of electric potential between controlling grid wires for  $U_{cg} = 20$  kV, 25 kV, 30 kV,  $U_{ca} = 120$  kV,  $r_g = 0.1$  m.

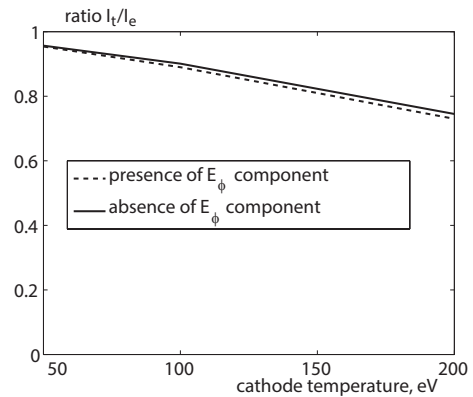


Figure 4: Dependence of the efficiency of the electron beam focusing to the target on the cathode plasma temperature and azimuthal electric field in the controlling grid region for  $U_{ca} = 120$  kV,  $U_{cg} = 30$  kV,  $r_g = 0.1$  m

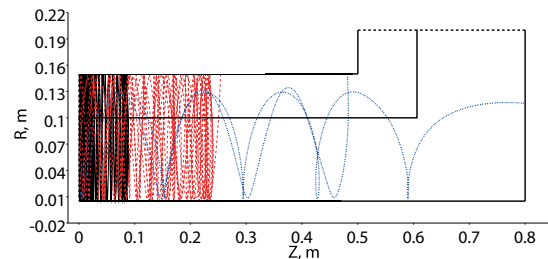


Figure 5: Examples of oscillating electron trajectories for  $U_{ca} = 120$  kV,  $U_{cg} = 20$  kV,  $r_g = 0.1$  m. Trajectory started near cathode center (black solid line), trajectory started near cathode edge (blue dash-dot line), trajectory started between center and edge of cathode (red dashed line).

The increase of the cathode plasma temperature results in the emission current and power density suppression, especially near the target center where the density of oscillating electrons is larger. Note that in the presence of oscillating electrons, some oscillation of the electron current in time is observed (see Fig. 7). There are two types of oscillations – low-frequency and high-frequency. As the analysis shows, the low-frequency oscillations appear in the presence of backscattered electrons and high-frequency oscillations – in the presence of passing electrons. From proposed results one can conclude that the required energy density of the electron beam on the target ( $40 \text{ J/cm}^2$ ) can be achieved under the following conditions:

- the cathode–grid voltage value is 23–25 kV;
- the temperature of the cathode plasma is less than 50 eV;
- beam pulse duration is 30–40  $\mu\text{s}$ ;
- the beam current is removed from both sides of the target.

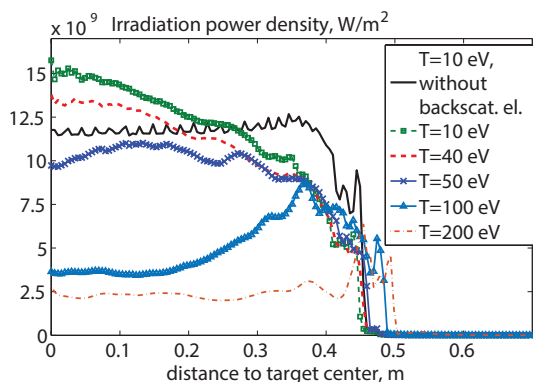


Figure 6: Power density on half of the target for different cathode temperatures for  $U_{ca} = 120 \text{ kV}$ ,  $U_{cg} = 20 \text{ kV}$ ,  $r_g = 0.1 \text{ m}$ .

## REFERENCES

- [1] V. I. Engelko, V. S. Kuznetsov, and G. Mueller. “Electron source of triode type with radial converging electron flow for irradiation of cylindrical targets”. In: *J. Appl. Phys.* 105 (2009).
- [2] R. Hockney and J. Eastwood. *Computer Simulation Using Particles*. Francis, 1988.
- [3] V. Altsybeyev et al. “Numerical simulation of a triode source of intense radial converging electron beam”. In: *Journal of Applied Physics* 120.14, 143301 (2016). DOI: <http://dx.doi.org/10.1063/1.4964335>.
- [4] V. V. Altsybeyev and V. A. Ponomarev. “Application of Gauss’s law space-charge limited emission model in iterative particle tracking method”. In: *Journal of Computational Physics* 324 (2016), pp. 62–72.
- [5] V. V. Altsybeyev. “Numerical Simulations of the Charged-Particle Flow Dynamics for Sources with a Curved Emission Surface”. In: *Physics of Particles and Nuclei Letters* 13.8 (2016), pp. 801–804.
- [6] V. Altsybeyev et al. “Numerical simulations of the radial convergent electrons and ions flows for cylindrical pulsed source”. In: *Stability and Control Processes in Memory of V.I. Zubov (SCP), 2015 International Conference*. 15637218. 2015, pp. 138–141.
- [7] V. Altsybeyev and V. Ponomarev. “Development of 2D Poisson equation C++ finite-difference solver for particle-in-cell method”. In: *Stability and Control Processes in Memory of V.I. Zubov (SCP), 2015 International Conference*. 15637294. 2015, pp. 195–197.
- [8] V. Altsybeyev et al. “Numerical simulations of the radial electron flow formation for the triode type source”. In: *10th International Vacuum Electron Sources Conference, IVESC 2014 and 2nd International Conference on Emission Electronics, ICEE 2014*. 6891934. 2014.
- [9] V. Engelko et al. “Influence of electrons reflected from a target on the operation of triode-type electron sources”. In: *J. Appl. Phys.* 88.7 (2000), pp. 3879–3888.
- [10] B. V. Oliver, T. C. Genoni, and D. V. Rose. “Space-charge limited currents in coaxial diodes with electron backscattering”. In: *J. Appl. Phys.* 90.10 (2001), pp. 4951–4956.

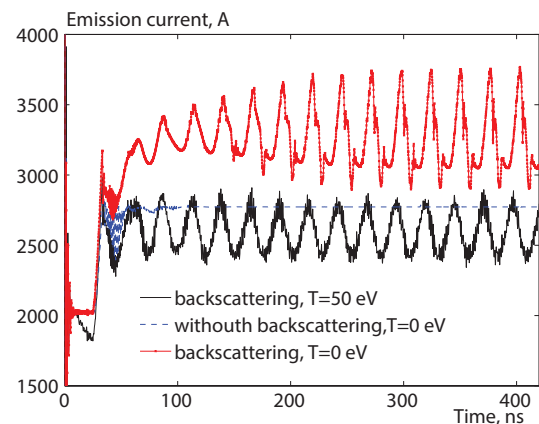


Figure 7: Dependence of emission currents on time for  $U_{ca} = 120 \text{ kV}$ ,  $U_{cg} = 20 \text{ kV}$ ,  $r_g = 0.1 \text{ m}$ ,  $T = 50 \text{ eV}$ .